World Journal of Nano Science and Engineering, 2014, 4, 58-69
Published Online June 2014 in SciRes. http://www.scirp.org/journal/wjnse
http://dx.doi.org/10.4236/wjnse.2014.42009

Scientific Research

Synthesis and Characterization of Some Selenium Nanometric Compounds: Spectroscopic, Biological and Antioxidant Assessments

Aly H. Atta[1,2*], Ahmed I. El-Shenawy[1,3], Fathy A. Koura[1,4], Moamen S. Refat[5,6]

[1]Department of Chemistry, Faculty of Education, University of Dammam, Dammam, KSA
[2]Department of Chemistry, Faculty of Science, Suez University, Suez, Egypt
[3]Department of Chemistry, Faculty of Science, Benha University, Benha, Egypt
[4]Department of Chemistry, Faculty of Science, Al-Azhar University, Cairo, Egypt
[5]Department of Chemistry, Faculty of Science, Taif University, Al-Hawiah, KSA
[6]Department of Chemistry, Faculty of Science, Port Said University, Port Said, Egypt
Email: *aly_atta@yahoo.com

Received 29 March 2014; revised 29 April 2014; accepted 6 May 2014

Abstract

Selenium (IV) vitamin A complex as antioxidant drug design was prepared and characterized by microanalysis, conductance, infrared spectra, Raman laser spectra, ^{1}HNMR spectra, scanning electron microscopy (SEM), X-ray powder diffraction (XRD) and thermogravimetric (TG/DTG and DTA) tool of analyses. Vitamin A chelate was coordinated as a mono-dentate ligand through the oxygen atom of –OH hydroxyl group. Thermal degradation analyses discussed the removal of terminal methyl molecules in the first and second decomposition stage while the organic ligand moieties existed in the third and subsequence steps. The Se (IV) complex in comparable with free vitamin A ligand has been assessed against some kinds of bacteria and fungi which gave a significant inhibition. The surface morphology and nano scale size of selenium metal and its vitamin complex were proved. The activation energy and other thermodynamic parameters (ΔH^*, ΔS^* and ΔG^*) of Se (IV) complex were calculated using Coats-Redfern and Horowitz-Metzger equations.

Keywords

Vitamin A, Selenium, Nano-Scale, Spectroscopic, Thermal Analysis, Antimicrobial Activity

*Corresponding author.

How to cite this paper: Atta, A.H., *et al.* (2014) Synthesis and Characterization of Some Selenium Nanometric Compounds: Spectroscopic, Biological and Antioxidant Assessments. *World Journal of Nano Science and Engineering*, **4**, 58-69.
http://dx.doi.org/10.4236/wjnse.2014.42009

1. Introduction

Selenium element was mentioned important due to its interesting role in the life construction of plants and biological systems, which absorb organoselenium compounds accumulated in the soils [1] [2]. It is an essential nutrient at trace level but toxic in excess [3]. Selenium is a trace mineral that is essential to good health but required only in small amounts [4]. Selenium is incorporated into proteins to make selenoproteins, which are important as antioxidant enzymes that help to prevent cellular damage from free radicals and to the development of chronic diseases such as cancer and heart disease [5]. Other selenoproteins help to regulate thyroid function and play a role in the immune system [6]. Because of its antioxidant role, selenium has been studied for its potential to protect the body from many degenerative diseases, including Parkinson's and cancer [7]. Vitamin A (**vit-OH**; **Figure 1**) is an essential nutrient for human body. The vitamin A has biological activities [8]. Vitamin A deficiency was a major nutritional deficiency disorder in many developing countries, especially affects young children, in whom it can cause xerophthalmia and lead to blindness, and can also limit growth, weaken innate and acquired host defenses, exacerbate infection and increase the risk of death [9]. Generally, metal ions were required for many critical functions in humans [10]-[12]. The ability to recognize to the molecular level and to treat diseases caused by inadequate metal-ion function constitutes an important aspect of medicinal bioinorganic chemistry [10] [12]. Metal complexes have been playing a key role in the development of modern chemotherapy [13], for example, complexation of non-steroidal anti-inflammatory drugs to copper overcomes some of the gastric side effects of these drugs [14]. The release of cytotoxins such as nitrogen mustards from redox-active metals such as cobalt in the hypoxic regions of solid tumors has the potential to improve drug activity and reduce toxicity [15]. The metal based drugs were also being used for the treatment of a variety of ailments viz. diabetes, rheumatoid arthritis, inflammatory and cardiovascular diseases as well as diagnostic [16]. A number of drugs and potential pharmaceutical agents also contain metal-binding and potentially influence their bioactivities [17]-[19]. Metal-organic frameworks were a burgeoning field in the last two decades, not only stems from their tremendous potential applications in areas such as catalysis, molecular adsorption, magnetism, nonlinear optics, and molecular sensing, but also from their novel topologies and intriguing structural diversities [20] [21]. On the other hand, many organic drugs, which possess modified pharmacological and toxicological properties administered in the form of metallic complexes [22], have the potential to act as ligands and the resulting metal-drug complexes are particularly important both in coordination chemistry and biochemistry [23] [24], however, the study of metal-drug complexes is still in its early stages, thus representing a great challenge in current synthetic chemistry and coordination chemistry. Recently, the trend of metal drug complexes has significant interest in order to achieve an enhanced therapeutic effect in combination with decreased toxicity. To the best of our knowledge, little attentions have been made to discuss the interaction between vitamin A and selenium (IV) metal ions and the literature is still poor in such spectroscopic characterizations. The interpretation is based on the ability of the cited drug to form complex associate with vital antioxidant metal ions like Se (IV). The spectral characteristic and the stability of the formed complex were also discussed.

2. Experimental

All chemicals used throughout this study were Analar or extra pure grade and received from Aldrich chemical company.

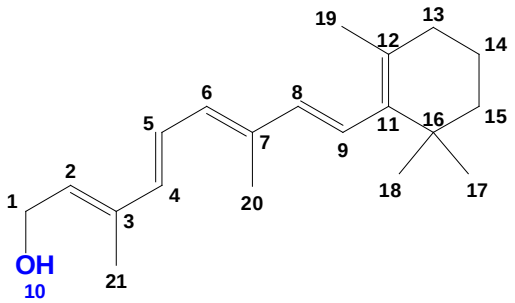

Figure 1. 3, 7-Dimethyl-9-(2, 6, 6-trimethyl-cyclohex-1-enyl)-nona-2, 4, 6, 8-tetraen-1-ol (Vitamin A; vit-OH).

2.1. Preparation of Selenium Nano Particles

The Se metal nano particles was prepared previously [25] by mixing equal volumes of aqueous solutions of 0.01 M of SeO_2 with 0.1 M of acetamide as following equation.

$$SeO_2 + CH_5CON + H_2O \xrightarrow{90^\circ C} Se + 2CO + NH_3 + 2H_2O$$

The mixture was heated on a water bath to approximately 90˚C for about ~24 hrs. The precipitate filtered off, washed several times with bidistilled water and dried in *vacuo* over $CaCl_2$. The selenium metal product was received in powder solid form. The elemental analysis for the obtained product shows the absence of carbon and nitrogen elements. The yield of selenium was ~70%.

2.2. Preparation of Solid Selenium (IV) vit-OH Complex

A mixture of solid powder of selenium metal (1 mmole) and the **vit-OH** (4 mmole) in toluene solvent (50 mL) was refluxed for 12 hr at 60˚C. The un-reacted of selenium metal powder was removed by filtration, and the resultant brownish red solution were reduced to *ca*. 1/3 of its volume and cooled to room temperature. The solid brown complex obtained was then collected by filtration, washed with little amount of toluene and dried in *vacuo* over anhydrous calcium (II) chloride. Elemental analysis, Calculated: %C = 78.45, %H = 9.88, %Se = 6.45; Found: %C = 78.32, %H = 9.56, %Se = 6.31.

2.3. Instrumental Analyses

The elemental analyses of carbon, and hydrogen contents were performed using a Perkin Elmer CHN 2400 (USA). The molar conductivities of freshly prepared 1.0×10^{-3} mol/cm^3 dimethylsulfoxide (DMSO) solutions were measured for the dissolved compounds using Jenway 4010 conductivity meter. The electronic absorption spectrum of Se (IV) complex was recorded in DMSO solvent within 600 - 200 nm range using a UV2 Unicam UV/Vis Spectrophotometer fitted with a quartz cell of 1.0 cm path length. The infrared spectra with KBr discs were recorded on a Bruker FT-IR Spectrophotometer (4000 - 400 cm^{-1}). Raman laser of samples were measured on the Bruker FT Raman with laser 50 mW. The ^{1}H-NMR spectra were recorded on Varian Mercury VX-300 NMR spectrometer. ^{1}H spectra were run at 300 MHz spectra in deuterated dimethylsulphoxide (DMSO-d_6). Chemical shifts are quoted in δ and were related to that of the solvents. The thermal studies TG/DTG-50H and DTA-50 H were carried out on a Shimadzu thermo-gravimetric analyzer under nitrogen till 800˚C. Scanning electron microscopy (SEM) images were taken in Quanta FEG 250 equipment. The X-ray diffraction patterns for the complexes were recorded on X 'Pert PRO PANanalytical X-ray powder diffraction, target copper with secondary monochromate.

2.4. Antimicrobial Test

According to Gupta *et al*., 1995 [26], the hole well method was applied. The investigated isolates of bacteria and fungi seeded in tubes with nutrient broth (NB) and Dox's broth (DB), respectively. The seeded (NB) for bacteria and (DB) for fungi (1 ml) were homogenized in the tubes with 9 ml of melted (45˚C) nutrient agar (NA) for bacteria and (DA) for fungi. The homogenous suspensions poured into Petri dishes. The holes (diameter 0.5 cm) done in the cool medium. After cooling in these holes, about 100 µl of the investigated compounds applied using a micropipette. After incubation for 24 h in an incubator at 37˚C and 28˚C for bacteria and fungi, respectively, the inhibition zone diameter were measured and expressed in cm. The antimicrobial activities of the investigated compounds were tested against some kinds of bacteria *as Escherichia coli* (Gram − ve) and *Staph albus* (Gram + ve) as well as some kinds of fungi as *Aspergillus flavus* and *Aspergillus niger*. In the same time with the antimicrobial investigations of the compounds, the pure solvent also tested. The concentration of each solution was 1.0×10^{-3} mol/L. Commercial DMSO was employed to dissolve the tested samples.

3. Results and Discussion

3.1. Characterization of Selenium Nano Scale

The formation of brown colored selenium metal in nano scale size was prepared upon the heating of an aqueous mixture of SeO_2 with acetamide at 90˚C. The isolated of selenium metal powder occurs during the decomposition

of acetamide according to the important role of metal ion on the decomposition process via aqueous media. The infrared spectrum of the SeO_2 with acetamide at 90˚C product is shown in **Figure 2**. The infrared spectrum of the obtained selenium metal product shows no bands due to characteristic groups of acetamide (carbonyl and amide groups). The XRD patterns of Se metal are shown in **Figure 3**. All definite peaks of Se metal are indexed as Se metal structure, which are matched and compared with the standard data. The SEM micrograph of the prepared Se metal is shown in **Figure 4**. The average grain size of selenium metalwere calculated and found in between 0.65 µm. From **Figure 4** it is so difficult to observe inhomogeneitiy within the same micrograph due to that the solution route synthesis with acetamide precursor is very fine and the particle size must be in nano-range. The grain size for nano compounds were calculated according to Scherrer's formula [27].

$$B = 0.87\,\lambda / D\cos\theta$$

where D is the crystalline grain size in nm, θ, half of the diffraction angle in degree, λ is the wavelength of X-ray source (Cu-K_∞) in nm, and B, degree of widening of diffraction peak which is equal to the difference of full width at half maximum (FWHM) of the peak at the same diffraction angle between the measured sample and standard one.

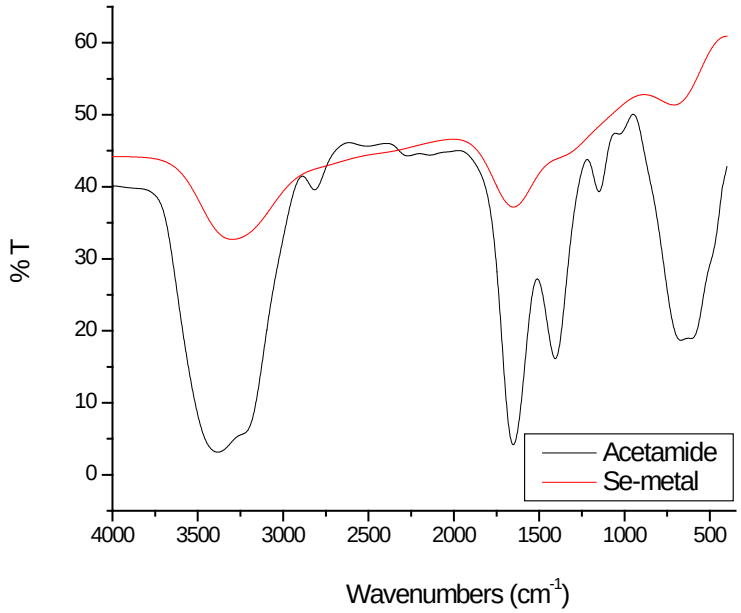

Figure 2. Infrared spectra of acetamide as a free ligand and Se metal.

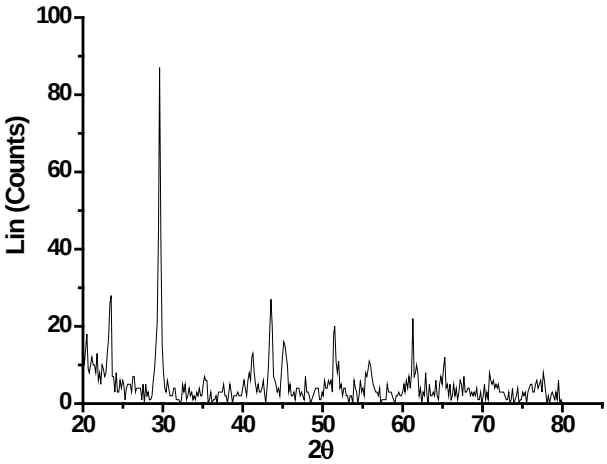

Figure 3. XRD spectrum of the resulted Se metal.

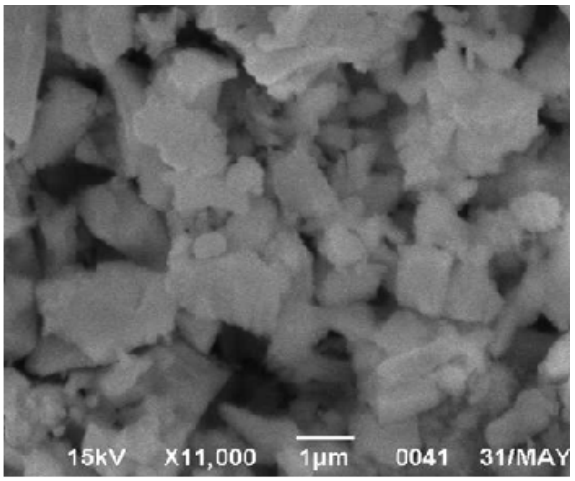

Figure 4. SEM micrographs of Se metal.

The Raman laser spectrum of Se metal is reported in **Figure 5**. For the pure selenium sample the spectrum is characterized by a strong band at 237 cm^{-1} which is attributed to the vibrational mode of –Se-Se-Se-chains [28] [29]. Additional weaker features can be revealed at 141 cm^{-1} which are assigned to the presence of Se_8 rings and to the bending modes of Se units.

3.2. Characterization of Selenium (IV) Vitamin A Complex

The reaction of **vit-OH** with selenium (0) metal in toluene solvent gave a brown colored solid complex. The found and calculated percentage of elemental analysis is in a well agreement with each other and proves the suggested molecular formula of the resulted selenium complex with molar ratio 1:4 (Se: **vit-OH**). The complexes have high melting points ~220˚C. The molar conductivity of selenium complex in DMSO has 15 $\Omega^{-1}\cdot cm^2\cdot mol^{-1}$, so that, it is non-electrolytes nature [30] [31]. Vitamin A ligand behaves as monodentate ligand and coordinates to selenium metal through the oxygen of hydroxyl group.

3.2.1. Electronic Absorption Spectra

The formation of the Se-**vit-OH** complex was also confirmed by UV-Vis spectroscopic technique. **Figure 6**, show the electronic absorption spectrum of the complex in DMSO in the 200 - 600 nm range. It can see that the free vitamin A has one distinct absorption band at 350 nm which may be attributed to $n \rightarrow \pi^*$ intra-ligand transition. In the spectra of the selenium complex this band is blue shifted clearly to 310 nm, where the complex show two bands at 239 and 310 nm assigned to $\pi \rightarrow \pi^*$ and $n \rightarrow \pi^*$ respectively, suggesting the ligand is binding to selenium metal through the lone pair of electrons on oxygen atom of –OH group. The electronic absorption spectrum of the selenium complex in DMSO solution has significant band at 370 nm due to the charge transfer transition from metal-to-ligand.

3.2.2. Infrared Spectra

The infrared spectra of **vit-OH** free ligand and its selenium complex were recorded in **Figure 7**. The spectra are similar but there are some differences which could give indication on the type of coordination. The IR spectrum of **vit-OH** shows a very strong broad band at 3406 cm^{-1} which assigned to ν(O-H) stretching vibration of alcoholic OH group, ionization of the alcoholic OH group with subsequent ligation through oxygen atom seems a plausible explanation [32]. To ascertain the involvement of ν(OH) of alcoholic group of **vit-OH** in the coordination process to be followed the stretching vibration bands of ν(C-O) in selenium **vit-OH complex**, the examination of this complex show that the ν(C-O) is shifted to lower wavenumber from 1073 and 1176 cm^{-1} in case of free ligand to 1084 and 1143 cm^{-1} in the complex. This result indicates that the alcoholic group is participated in the complexation [33] and the **vit-OH** acts as monodentate ligand. The **vit-OH** complex show two weak bands observed at 2955 and 2929 cm^{-1} which assigned to the stretching vibration of ν(C-H) of CH_3 and CH_2 groups. Involvement of the oxygen atoms of hydroxyl group are also confirmed by the presence of new bands in the selenium complex at 520 and 488 cm^{-1} due to the ν(M-O) stretching vibrations respectively [34].

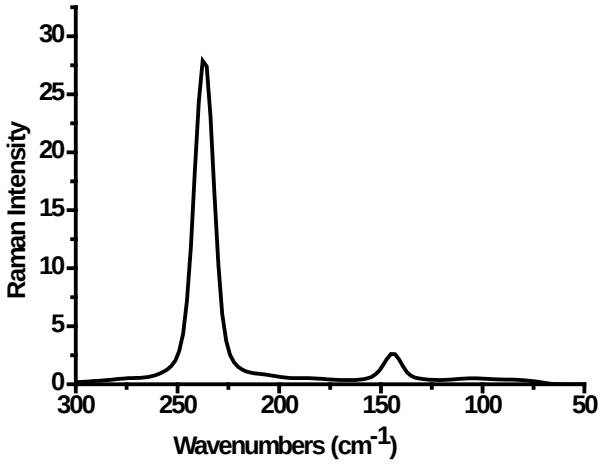

Figure 5. Raman laser spectrum of Se metal.

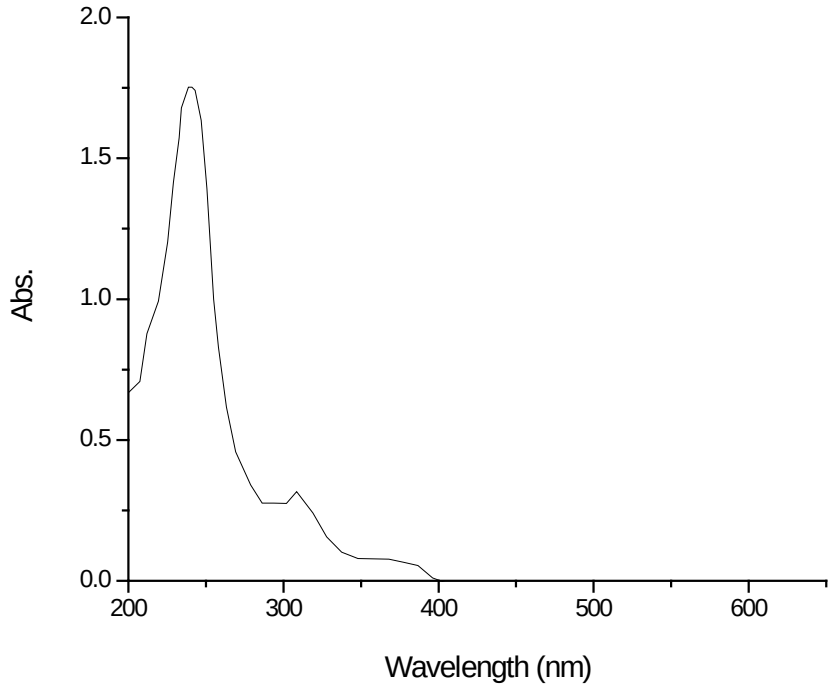

Figure 6. UV-vis electronic spectrum of Se-**vit-OH** complex.

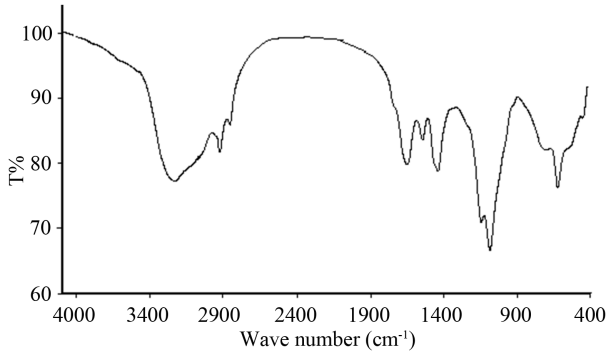

Figure 7. Infrared spectrum of Se-**vit-OH** complex.

3.2.3. ^{1}H-NMR Spectra

The ^{1}H-NMR data of **vit-OH** and its Se (0) complex is shown in **Figure 8**. ^{1}H-NMR spectrum of **vit-OH** show the signal at δ = ~ 9 ppm, which assigned to the proton of alcoholic OH group that is disappear in the Se-**vit-OH** complex. The disappearance of the signal of the proton of the hydroxyl group in the ^{1}H-NMR spectrum of the complex confirms that the hydroxyl group contribute in the complexation between **vit-OH** and Se (0) metal [35]. The proton NMR spectrum for Se (0) complex shows a singlet peaks at 1.30, 3.20 and 4.50 ppm. These peaks are assigned to protons of -CH_3, -CH_2, and =CH groups, supporting the complex formula as suggested in **Figure 9**.

3.2.4. Thermal Analysis

The obtained Se-**vit-OH** complex was studied by thermogravimetric TG/DTG and DTA differential thermal analysis from ambient temperature to 800˚C under N_2 atmospheres. The TG curves were redrawn as mg mass loss versus temperature and DTG curve was redrawn as rate of loss of mass versus temperature (**Figure 10** and **Figure 11**). The thermal decomposition of [Se(**vit-OH**)$_4$] complex occurs at four decomposition steps. The first degradation step takes place within a temperature range of 50˚C - 120˚C at DTG_{max} = 80˚C and it correspond to the loss of three terminal methyl groups with an observed weight loss 3.30% (calcd. = 3.67%). The second decomposition step occur within temperature range 120˚C - 225˚C at DTG_{max} = 185˚C and DTA = 195˚C (exothermic) that assigned to the loss of another 14CH_3 molecules with a weight loss (obs =17.50%, calcd. = 17.15%). The third step occur within temperature range 225˚C - 330˚C at DTG_{max} = 285˚C and DTA= 300˚C (exothermic) due to the loss of $C_{22}H_{22}O_4$ organic molecule with mass loss (obs. = 28.65%, calcd. = 28.58%). The fourth step occur within a temperature range 330˚C - 435˚C at DTG_{max} = 365˚C and DTA = 370˚C (exo) due to the loss of $C_{23}H_{47}$ (organic moiety) with a mass loss (obs. = 26.60%, calcd. = 26.37%). The Se-metal contaminated with polluted carbon atoms remains as final residual till 800˚C.

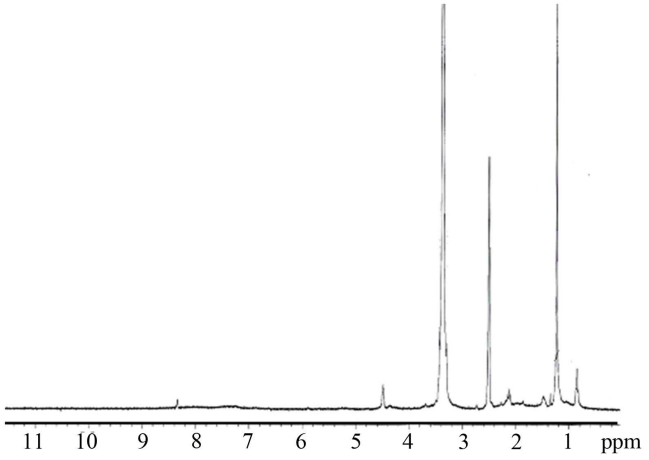

Figure 8. ^{1}HNMR spectrum of Se-**vit-OH** complex.

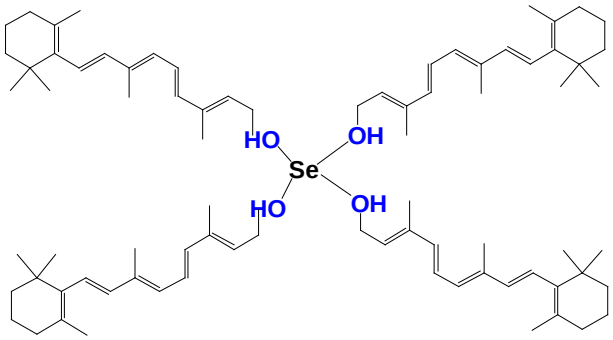

Figure 9. Suggested structure of Se-**vit-OH** complex.

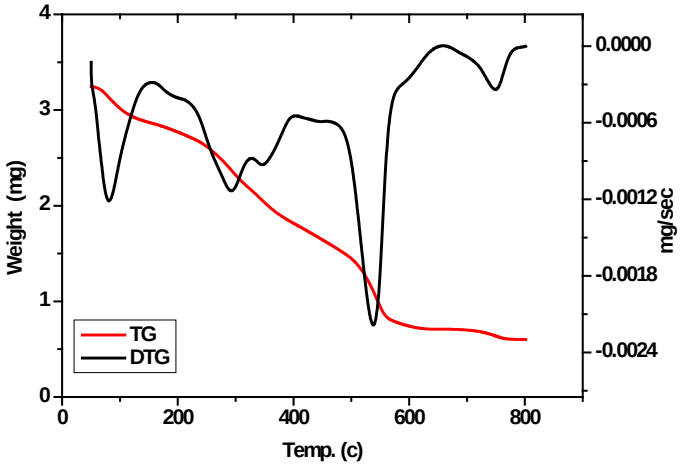

Figure 10. TG/DTG curves of Se-**vit-OH** complex.

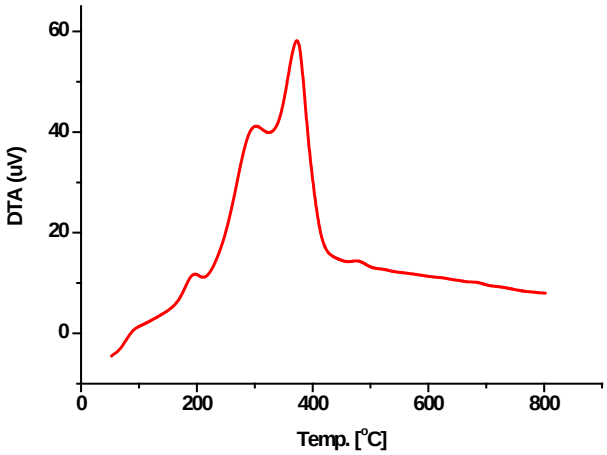

Figure 11. DTA curve of Se-**vit-OH** complex.

3.2.5. Kinetic Studies

Most commonly used methods are the differential method of Freeman and Carroll [36] integral method of Coat and Redfern [37] and the approximation method of Horowitz and Metzger [38]. In the present investigation, the general thermal behaviors of the vitamin A comple in terms of stability ranges, peak temperatures and values of kinetic parameters are discussed. The kinetic parameters have been evaluated using the Coats-Redfern equation:

$$\int_0^{\alpha} \frac{d\alpha}{(1-\alpha)^n} = \frac{A}{\varphi}\int_{T_1}^{T_2} \exp\left(-\frac{E^*}{RT}\right)\mathrm{dt} \tag{1}$$

This equation on integration gives:

$$\ln\left[-\frac{\ln(1-\alpha)}{T^2}\right] = -\frac{E^*}{RT} + \ln\left(\frac{AR}{\varphi E^*}\right) \tag{2}$$

where φ is the linear heating rate, R is the gas constant, T is the DTG temperature peak, α, is the fraction of the sample decomposed at time t, A is the pre-exponential factor. A plot of left-hand side against $1/T$ was drawn. E^* is the energy of activation in $J \cdot mol^{-1}$ and calculated from the slop and A in (s^{-1}) from the intercept value. The entropy of activation ΔS^* in ($JK^{-1} \cdot mol^{-1}$) was calculated by using the equation:

$$\Delta S^* = R \cdot \ln\left(Ah/k_B T_s\right) \tag{3}$$

where k_B is the Boltzmann constant, h is the Plank's constant and T_s is the DTG peak temperature [39].

The Horowitz-Metzger equation is an illustrative of the approximation methods.

$$\log\left[\left\{1-(1-\alpha)^{1-n}\right\}\Big/(1-n)\right] = E^{*}\theta/2.303RT_s^{2} \quad \text{for } n \neq 1 \tag{4}$$

When $n = 1$, the LHS of equation 4 would be $\log[-\log(1-\alpha)]$. For a first-order kinetic process the Horowitz-Metzger equation may be written in the form:

$$\log\left(\log\left(w_\alpha/w_\gamma\right)\right) = E^{*}\theta/2.303RT_s^{2} - \log 2.303$$

where $\theta = T - T_s$, $w_\gamma = w_\alpha - w$, w_α = mass loss at the completion of the reaction. The plot of $\log[\log(w_\alpha/w_\gamma)]$ vs θ was drawn and found to be linear from the slope of which E^{*} was calculated. The pre-exponential factor, A, was calculated from the equation:

$$E^{*}/RT_s^{2} = A\Big/\left[\varphi\exp\left(-E^{*}/RT_s\right)\right]$$

The entropy of activation, ΔS^{*}, was calculated from Equation (3). The enthalpy activation, ΔH^{*}, and Gibbs free energy, ΔG^{*}, were calculated from; $\Delta H^{*} = E^{*} - RT$ and $\Delta G^{*} = \Delta H^{*} - T\Delta S^{*}$, respectively. The kinetic parameters such as activation energy (ΔE^{*}), enthalpy (ΔH^{*}), entropy (ΔS^{*}) and free energy change of the decomposition (ΔG^{*}) have been evaluated graphically as shown in **Figure 12** and **Figure 13** by employing the Coats-Redfern

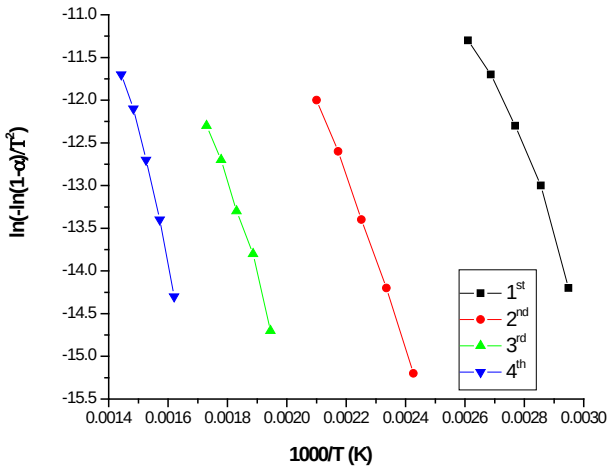

Figure 12. Coats-Redfern plots of the first, second, third and fourth thermal decomposition steps of Se-**vit-OH** complex.

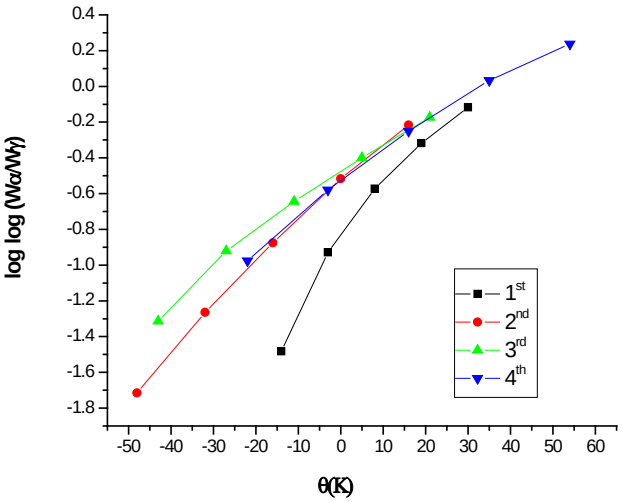

Figure 13. Horowitz-Metzger plots of the first, second, third and fourth thermal decomposition steps of Se-**vit-OH** complex.

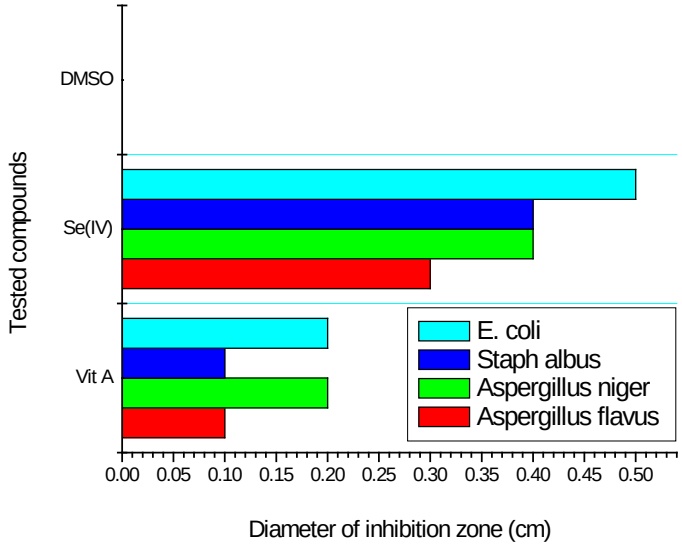

Figure 14. Biological evaluation of **vit-OH**, **Se-vit-OH** complex and DMSO solvent.

and Horwitz-Mitzger relations. The most significant result is the considerable thermal stability of the Se-**vit-OH** complex reflected from the high values of the activation energy of the decomposition. The entropy change ΔS^* of the formation activated complex from the starting reactants is in most cases of negative values. The negative sign of the ΔS^* suggests that the thermodynamic behavior is non-spontaneous (more ordered) reactions and the degree of structural "complexity" (arrangement, "organization") of the activated complex was lower than that of the starting reactants, also the thermodynamic behavior of selenium complex is endothermic reactions ($\Delta H > 0$) and endergonic ($\Delta G > 0$), during the reactions. The thermodynamic data obtained with the two methods are in harmony with each other. The correlation coefficients of the Arrhenius plots of the thermal decomposition steps were found to lie in the range 0.97 to 0.99, showing a good fit with linear function.

3.2.6. Antimicrobial Assessment of Se-vit-OH Complex

Peng *et al*. [40] reported that 36 nm of Se metal has lower toxicity than selenite or selenomethionine with higher particle sizes, but all of these forms of (Se) possess similar ability to increase selenoenzyme levels. They deduced also that the size of nanoparticles plays an important role in their biological activity: as expected, from range 5 - 200 nm for Se which can be directly scavenge free radicals *in vitro* in a size-dependent fashion. Accordingly the present techniques of synthesizing selenium metal within the range of (15 - 35 nm) is a unique and pioneer to increase the validity for selenium in biological reaction and leading new trends to decrease toxicity of selenium of higher particle size as reported in literature [40]. Antibacterial and antifungal activities of Se-**vit-OH** complex are carried out against some kinds of bacteria as *Escherichia coli* (Gram − ve) and *Staphalbus* (Gram + ve) as well as some kinds of fungi as *Aspergillus niger* and *Aspergillus flavus*. The antimicrobial activity was estimated based on the size of inhibition zone around dishes. The free vitamin A was found to have the lowest activity against four types of bacteria and fungi, while the selenium complex was found to be more potent than the original chelate in their inhibition properties (**Figure 14**). This has been explained in terms of the greater lipid solubility and cellular penetration of the complexes [41] [42].

Acknowledgements

This work was funded By Deanship of Scientific Research at the University of Dammam, Kingdom Saudi Arabia under Project Grants No. 2013173.

References

[1] Odom, J.D., Dawson, W.H. and Ellis, P.D. (1979) Selenium-77 Relaxation Time Studies on Compounds of Biological Importance: Dialkyl Selenides, Dialkyl Diselenides, Selenols, Selenonium Compounds, and Seleno Oxyacids. *Journal*

of the American Chemical Society, **101**, 5815-5822. http://dx.doi.org/10.1021/ja00513a058

[2] Robberecht, H.J. and Deelstra, H.A. (1984) Selenium in Human Urine Determination, Speciation and Concentration Levels. *Talanta*, **31**, 497-508. http://dx.doi.org/10.1016/0039-9140(84)80129-0

[3] Andrews, R.W. and Johnson, D.C. (1975) Voltammetric Deposition and Stripping of Selenium(IV) at a Rotating Gold-Disk Electrode in 0.1M Perchloric Acid. *Analytical Chemistry*, **47**, 294-299. http://dx.doi.org/10.1021/ac60352a005

[4] Thomson, C.D. (2004) Assessment of Requirements for Selenium and Adequacy of Selenium Status: A Review. *European Journal of Clinical Nutrition*, **58**, 391-402. http://dx.doi.org/10.1038/sj.ejcn.1601800

[5] Combs, G.F. and Gray, W.P. (1998) Chemopreventive Agents: Selenium. *Pharmacology & Therapeutics*, **79**, 179-192. http://dx.doi.org/10.1016/S0163-7258(98)00014-X

[6] Levander, O.A. (1997) Nutrition and Newly Emerging Viral Diseases: An Overview. *Journal of Nutrition*, **127**, 948S-950S.

[7] Corvilain, B., Contempre, B., Longombe, A.O., Goyens, P., Gervy-Decoster, C., Lamy, F., Vanderpas, J.B. and Dumont, J.E. (1993) Selenium and the Thyroid: How the Relationship Was Established. *The American Journal of Clinical Nutrition*, **57**, 244S-248S.

[8] Sauberlich, H.E., Hodges, R.E., Wallace, D.L., Kolder, H., Canham, J.E., Hood, J., Raica Jr., N. and Lowry, L.K. (1974) A Metabolism and Requirements in the Human Studied with the Use of Labeled Retinol. *Vitamins and Hormones*: *Advances on Research and Applications*, **32**, 251.

[9] Sommer, A. and West, K.P. (1996) Vitamin A Deficiency: Health, Survival, and Vision. Oxford University Press, New York, 100-116.

[10] Drevensek, P., Zupancic, T., Pihlar, B., Jerala, R., Kolitsch, U., Plaper, A. and Turel, I. (2005) Mixed-Valence Cu(II)/Cu(I) Complex of Quinolone Ciprofloxacin Isolated by a Hydrothermal Reaction in the Presence of l-Histidine: Comparison of Biological Activities of Various Copper-Ciprofloxacin Compounds. *Journal of Inorganic Biochemistry*, **99**, 432-442. http://dx.doi.org/10.1016/j.jinorgbio.2004.10.018

[11] He, J.H., Xiao, D.R., Chen, H.Y., Yan, S.W., Sun, D.Z., Wang, X., Yang, J., Yuan, R. and Wang, E.B. (2012) Two Novel Entangled Metal-Quinolone Complexes with Self-Threading and Polythreaded Characters. *Inorganica Chimica Acta*, **385**, 170-177. http://dx.doi.org/10.1016/j.ica.2012.01.056

[12] Kathawate, L., Sproules, S., Pawar, O., Markad, G., Haram, S., Puranik, V. and Salunke-Gawali, S. (2013) Synthesis and Molecular Structure of a Zinc Complex of the Vitamin K_3 Analogue Phthiocol. *Journal of Molecular Structure*, **1048**, 223-229. http://dx.doi.org/10.1016/j.molstruc.2013.05.057

[13] Gielen, M. and Tiekink, E.R.T. (2005) Metallotherapeutic Drugs and Metal-Based Diagnostic Agents, the Use of Metals in Medicine. Wiley, Chichester. http://dx.doi.org/10.1002/0470864052

[14] Weder, J.E., Dillon, C.T., Hambley, T.W., Kennedy, B.J., Lay, P.A., Biffin, J.R., Regtop, H.L. and Daview, N.M. (2002) Copper Complexes of Non-Steroidal Anti-Inflammatory Drugs: An Opportunity Yet to Be Realized. *Coordination Chemistry Reviews*, **232**, 95-126. http://dx.doi.org/10.1016/S0010-8545(02)00086-3

[15] Ware, D.C., Brothers, P.J. and Clark, G.R. (2000) Synthesis, Structures and Hypoxia-Selective Cytotoxicity of Cobalt(III) Complexes Containing Tridentate Amine and Nitrogen Mustard Ligands. *Journal of the Chemical Society, Dalton Transactions*, **6**, 925-932. http://dx.doi.org/10.1039/a909447d

[16] Nakai, M., Sekiguchi, F., Obata, M., Ohtsuki, C., Adachi, Y., Sakurai, H., Orvig, C., Rehder, D. and Yano, S. (2005) Synthesis and Insulin-Mimetic Activities of Metal Complexes with 3-Hydroxypyridine-2-Carboxylic Acid. *Journal of Inorganic Biochemistry*, **99**, 1275-1282. http://dx.doi.org/10.1016/j.jinorgbio.2005.02.026

[17] Muller, J.G. and Burrows, C.J. (1998) Metallodrug Complexes That Mediate DNA and Lipid Damage via Sulfite Autoxidation: Copper(II) Famotidine and Iron(III) Bis(Salicyglycine). *Inorganica Chimica Acta*, **275-276**, 314-319. http://dx.doi.org/10.1016/S0020-1693(97)06179-3

[18] Duda, A.M., Kowalik-Jankowska, T., Kozlowski, H. and Kupka, T. (1995) Histamine H_2 Antagonists: Powerful Ligands for Copper(II). Reinterpretation of the Famotidine-Copper(II) System. *Journal of the Chemical Society, Dalton Transactions*, No. 17, 2909-2913. http://dx.doi.org/10.1039/dt9950002909

[19] Kubiak, M., Duda, A.M., Ganadu, M.L. and Kozlowski, H. (1996) Crystal Structure of a Copper(II)-Famotidine Complex and Solution Studies of the Cu^{2+}-Famotidine-Histidine Ternary System. *Journal of the Chemical Society, Dalton Transactions*, No. 9, 1905-1908. http://dx.doi.org/10.1039/dt9960001905

[20] Wu, C.-D., Lu, C.-Z., Zhuang, H.-H. and Huang, J.-S. (2002) Hydrothermal Assembly of a Novel Three-Dimensional Framework Formed by $[GdMo_{12}O_{42}]^{9-}$ Anions and Nine Coordinated Gd^{III} Cations. *Journal of the American Chemical Society*, **124**, 3836-3837. http://dx.doi.org/10.1021/ja017782w

[21] Dybtsev, D.N., Chun, H. and Kim, K. (2004) Rigid and Flexible: A Highly Porous Metal-Organic Framework with Unusual Guest-Dependent Dynamic Behavior. *Angewandte Chemie International Edition*, **43**, 5033-5036. http://dx.doi.org/10.1002/anie.200460712

[22] López-Gresa, M.P., Ortiz, R., Perelló, L., Latorre, J., Liu-González, M., García-Grand, S., Pérez-Priede, M. and Cantón, E. (2002) Interactions of Metal Ions with Two Quinolone Antimicrobial Agents (Cinoxacin and Ciprofloxacin): Spectroscopic and X-Ray Structural Characterization. Antibacterial Studies. *Journal of Inorganic Biochemistry*, **92**, 65-74. http://dx.doi.org/10.1016/S0162-0134(02)00487-7

[23] Xiao, D.-R., Wang, E.-B., An, H.-Y., Li, Y.-G. and Xu, L. (2007) Syntheses and Structures of Three Unprecedented Metal-Ciprofloxacin Complexes with Helical Character. *Crystal Growth & Design*, **7**, 506-512. http://dx.doi.org/10.1021/cg060492c

[24] Xiao, D.R., He, J.H., Sun, D.Z., Chen, H.Y., Yan, S.W., Wang, X., Yang, J., Yuan, R. and Wang, E.B. (2012) Three 3D Metal-Quinolone Complexes Based on Trimetallic or Rod-Shaped Secondary Building Units. *European Journal of Inorganic Chemistry*, **2012**, 1783-1789. http://dx.doi.org/10.1002/ejic.201101229

[25] Refat, M.S. and El-Sabawy, K.M. (2011) Infrared Spectra, Raman Laser, XRD, DSC/TGA and SEM Investigations on the Preparations of Selenium Metal, (Sb_2O_3, Ga_2O_3, SnO and HgO) Oxides and Lead Carbonate with Pure Grade Using Acetamide Precursors. *Bulletin of Materials Science*, **34**, 873-881. http://dx.doi.org/10.1007/s12034-011-0208-z

[26] Gupta, R., Saxena, R.K., Chatarvedi, P. and Virdi, J.S. (1995) Chitinase Production by *Streptomyces viridificans*: Its Potential in Fungal Cell Wall Lysis. *Journal of Applied Bacteriology*, **78**, 378-383. http://dx.doi.org/10.1111/j.1365-2672.1995.tb03421.x

[27] Scherrer, P. (1918) Bestimmung der Größe und der inneren Struktur von Kolloidteilchen mittels Röntgenstrahlen. *Nachrichten von der Gesellschaft der Wissenschaften zu Göttingen*, **2**, 98-100.

[28] Iovu, M.S., Kamitsos, E.I., Varsamis, C.P.E., Boolchand, P. and Popescu, M. (2005) Raman Spectra of $AsxSe_{100-X}$ and $As_{40}Se_{60}$ Glassesdoped with Metals. *Chalcogenide Letters*, **2**, 21-25.

[29] Kovanda, V., Vlček, M. and Jain, H. (2003) Structure of As-Se and As-P-Se Glasses Studied by Raman Spectroscopy. *Journal of Non-Crystalline Solids*, **326-327**, 88-92. http://dx.doi.org/10.1016/S0022-3093(03)00383-1

[30] Refat, M.S. (2007) Complexes of Uranyl(II), Vanadyl(II) and Zirconyl(II) with Orotic Acid "Vitamin B13": Synthesis, Spectroscopic, Thermal Studies and Antibacterial Activity. *Journal of Molecular Structure*, **842**, 24-37. http://dx.doi.org/10.1016/j.molstruc.2006.12.006

[31] Vogel, T. (1989) Vogel Textbook of Practical Organic Chemistry. 4th Edition, Wiley & Sons, Inc., New York, 133-325.

[32] Nakamoto, K. (1970) Infrared Spectra of Inorganic and Coordination Compounds. Wiley InterScience, New York.

[33] Mohamed, G.G., Zayed, M.A., Nour El-Dien, F.A. and El-Nahas, R.G. (2004) IR, UV-Vis, Magnetic and Thermal Characterization of Chelates of Some Catecholamines and 4-Aminoantipyrine with Fe(III) and Cu(II). *Spectrochimica Acta Part A*: *Molecular and Biomolecular Spectroscopy*, **60**, 1775-1781. http://dx.doi.org/10.1016/j.saa.2003.08.027

[34] Santi, E., Torre, M.H., Kremer, E., Etcheverry, S.B. and Baran, E. (1993) Vibrational Spectra of the Copper(II) and Nickel(II) Complexes of Piroxicam. *Vibrational Spectroscopy*, **5**, 285-293. http://dx.doi.org/10.1016/0924-2031(93)87004-D

[35] Arumuganathan, T., Srinivasarao, A., Kumar, T.V. and Das, S.K. (2008) Two Different Zinc(II)-Aqua Complexes Held Up by a Metal-Oxide Based Support: Synthesis, Crystal Structure and Catalytic Activity of $[HMTAH]_2[\{Zn(H_2O)_5\}\{Zn(H_2O)_4\}\{Mo_7O_{24}\}]\cdot 2H_2O$ (HMTAH = Protonated Hexamethylenetetramine). *Journal of Chemical Sciences*, **120**, 95-103. http://dx.doi.org/10.1007/s12039-008-0012-5

[36] Freeman, E.S. and Carroll, B. (1958) The Application of Thermoanalytical Techniques to Reaction Kinetics: The Thermogravimetric Evaluation of the Kinetics of the Decomposition of Calcium Oxalate Monohydrate. *The Journal of Physical Chemistry*, **62**, 394-397. http://dx.doi.org/10.1021/j150562a003

[37] Coats, A.W. and Redfern, J.P. (1964) Kinetic Parameters from Thermogravimetric Data. *Nature*, **201**, 68-69. http://dx.doi.org/10.1038/201068a0

[38] Horowitz, H.W. and Metzger, G. (1963) A New Analysis of Thermogravimetric Traces. *Analytical Chemistry*, **35**, 1464-1468. http://dx.doi.org/10.1021/ac60203a013

[39] Flynn, J.H.F. and Wall, L.A. (1966) General Treatment of the Thermogravimetry of Polymers. *Journal of Research of the National Bureau of Standards*, **70A**, 487-523. http://dx.doi.org/10.6028/jres.070A.043

[40] Peng, D.G., Zhang, J.S., Liu, Q.L. and Taylor, E.W. (2007) Size Effect of Elemental Selenium Nanoparticles (Nano-Se) at Supranutritional Levels on Selenium Accumulation and Glutathione S-Transferase Activity. *Journal of Inorganic Biochemistry*, **101**, 1457-1463. http://dx.doi.org/10.1016/j.jinorgbio.2007.06.021

[41] Jam, P. and Chaturvedi, K.K. (1976) Potentiometric Study of the Complexes of Sulphamethazine Salicylaldimine with Cu(II), Ni(II) and Co(II). *Journal of Inorganic and Nuclear Chemistry*, **38**, 799-800. http://dx.doi.org/10.1016/0022-1902(76)80359-4

[42] Jam, P. and Chaturvedi, K.K. (1977) Complexes of Cu(II), Ni(II) and Co(II) with Sulphamerazine. *Journal of Inorganic and Nuclear Chemistry*, **39**, 901-903. http://dx.doi.org/10.1016/0022-1902(77)80182-6